# Wobbling and Impairments-Aware Channel Model and its Implications on High-Frequency UAV Links

Morteza Banagar and Harpreet S. Dhillon

***Abstract*—This paper provides an impairments-aware unified channel model for the link between an unmanned aerial vehicle (UAV) and a ground user equipment (UE). In particular, we consider both physical and hardware impairments, where the former is unique to UAVs and refers to random physical vibrations of the UAV platform, also known as *wobbling*. The latter pertains to both the UAV and the UE and refers to intrinsic radio frequency (RF) impairments, such as power amplifier (PA) nonlinearity, phase noise, and in-phase/quadrature (I/Q) imbalance. We model the fluctuations of the UAV platform pitch angle (caused by wobbling) by a sinusoidal stochastic process. On the other hand, the combined effect of all hardware impairments is modeled by two wide-sense stationary (WSS) additive and multiplicative distortion noise processes, which is a well-accepted approach in the literature. Using this unified model, we characterize the autocorrelation function (ACF) of the impairments-aware channel impulse response, which further provides the coherence time of the channel. We also derive the power spectral density (PSD) of the distortion-plus-noise process of our unified channel model. To obtain useful insights from the joint impact of physical and hardware impairments on the air-to-ground wireless channel, we evaluate both of these metrics with reasonable impairment models and parameters. One key implication of our results is that the channel coherence time degrades noticeably at high frequencies even for small wobbling, which renders channel estimation of UAV links extremely challenging at these frequencies.**

***Index Terms*—UAV wobbling, hardware impairments, air-to-ground wireless channel, coherence time, power spectral density.**

## I. Introduction

As the UAV technology has matured over the past decade, the interest in using UAVs as aerial transceivers has skyrocketed due to many favorable features, such as agility and high probability of line-of-sight (LoS) [2]. However, this comes with challenges that are unique to UAVs. Primarily, because of not having fixed infrastructures and also natural phenomena such as wind gusts, UAV platforms may undergo random physical fluctuations, *albeit* small, which are called wobbling in the literature [3]. This random UAV wobbling, which is *unique* to aerial communications, may degrade the air-to-ground wireless channel quality, especially when the carrier frequencies are large (say more than 1 GHz). As another example, UAVs, similar to all terrestrial transceivers, suffer from RF imperfections (also known as hardware impairments) that deteriorate the performance of communication systems [4], [5]. Remarkably, the timely problem of the joint impact of UAV wobbling and hardware impairments on the air-to-ground wireless channel has not been investigated yet, which is the main focus of this paper. As a consequence, it is not immediately clear how these effects will manifest themselves in fundamental channel properties, such as the coherence time, which have important implications on the link design. Our results will also shed light on this important aspect.

*Related Works.* Analytical and empirical air-to-ground channel modeling have been a growing area of research over the past few years [6]–[10]. However, only a handful of them studied the effect of UAV wobbling or hardware impairments on the quality of the wireless channel. For instance, the authors in [11] studied the antenna gain mismatch problem due to random UAV wobbling for an aerial network. In [12], a stochastic model is introduced for UAV wobbling, using which the authors study resource allocation in aerial-terrestrial networks. The air-to-ground wireless channel performance in terms of coherence time is studied in [3], where the authors propose novel stochastic models for UAV wobbling and study both single-antenna and multiple-antenna scenarios. Along the similar lines as [3] and using the same random UAV wobbling models, the authors in [13] studied the impact of UAV wobbling on the Doppler effect at millimeter-wave (mmWave) frequencies. In a recent study, the measurement campaign in [14] has evaluated the impact of UAV wobbling on the channel, where the authors compared the received power variations between hovering and completely static UAVs. As for the hardware impairments, on the other hand, the volume of works is considerable. For instance, PA nonlinearity, phase noise, and I/Q imbalance have been separately studied in the literature (see e.g., [4], [15], [16] and the references therein). In particular, the *aggregate* effect of these three fundamental hardware impairments on the transmit and receive signals has been modeled in [4, Ch. 7], which has motivated many other analyses in communications theory. For example, a redefinition of two-hop relaying systems [17] with hardware impairments has been proposed in [18], where the authors derived the outage probability in these two-hop networks. In another seminal work from the same group [5], the authors proved the existence of a bound on the capacity of massive multiple-input multiple-output (MIMO) systems. Although the research on hardware impairments is mature, the volume of works on the impact of such impairments on the air-to-ground wireless channel is very sparse [19], and there is no work that studies the joint impact of UAV wobbling and hardware impairments on the channel, which is the main focus of this paper.

*Contributions and Outcomes.* In this paper, we propose an air-to-ground wireless channel model that is cognizant of different impairments associated with both the UAV and the UE. Considering a UAV-UE link in a multi-path environment with Rician fading, we study two different types of impairments: (i)

The authors are with Wireless@VT, Department of ECE, Virginia Tech, Blacksburg, VA. Email: {mbanagar, hdhillon}@vt.edu. The support of the US NSF (Grant CNS-1923807) is gratefully acknowledged. The extended journal version of this paper is available at [1].

physical, caused by random UAV wobbling, and (ii) hardware, caused by intrinsic RF nonidealities at both the UAV and the UE. We model UAV wobbling by a sinusoidal stochastic process, and model the hardware impairments by two WSS distortion noise processes. We then study the interplay between these two impairment types and their joint impact on the air-to-ground wireless channel. Specifically, we characterize the ACF of the proposed channel impulse response, using which we derive the channel coherence time and the PSD of the distortion-plus-noise process. Our analysis also reveals that the channel coherence time degrades significantly due to these impairments (especially wobbling) at higher frequencies (mmWave and higher), thereby requiring a higher number of pilots for channel estimation (eventually becoming prohibitive with increasing frequency). It is important to account for this much higher channel estimation overhead while proposing to use UAVs at higher frequencies. To the best of our understanding, this is the first work that provides a unified channel model for the air-to-ground wireless communications that accounts for both UAV wobbling and hardware impairments.

## II. System Model

We assume that a hovering UAV communicates with a ground UE in a multi-path environment with $N$ scatterers. As shown in Fig. 1 and without loss of generality, the UAV antenna is placed at a distance of $y_{\rm D}$ from the UAV centroid and has a distance of $d_0(t)$ and $d_i(t)$ from the ground UE and the $i$-th multi-path component (MPC) at time $t$, respectively. Furthermore, we represent the distance between the $i$-th MPC and the UE as $d_{{\rm S}_i,{\rm U}}$, and the angle-of-departure (AoD) from the UAV antenna to the $i$-th MPC as $\omega_i$, which is measured with respect to the $z$-axis.

In practice, an aerial-terrestrial communication link may suffer from various nonidealities, categorized in this paper as *physical* and *hardware* impairments and described next.

*Physical Impairments.* Unlike terrestrial base stations, UAVs do not have fixed infrastructures, which results in their physical fluctuations due to wind gusts, inclement weather conditions, or even high rotational speed of their rotors/propellers [3], [11], [20]. We refer to these small random physical vibrations of the UAV platform as wobbling, which has also been termed as jittering [12] and fluctuating [11] in the literature. As shown in Fig. 1, the wobbling pitch angle is denoted by $\theta(t)$ at time $t$. In this paper, we model UAV wobbling by a sinusoidal stochastic process defined as $\theta(t) = L\sin(2\pi Qt)$, where $L \sim U[-\theta_{\rm m}, \theta_{\rm m})$ and $Q \sim f_Q(q)$ are independent random variables that represent the amplitude and variation frequency of $\theta(t)$, respectively. In these equations, $\theta_{\rm m}$ is the maximum UAV pitch angle and $f_Q(.)$ is an arbitrary but known probability density function (pdf). Using the characteristic function (cf) of uniform random variables and defining $\mathrm{sinc}(x) = \frac{\sin(\pi x)}{\pi x}$, we have $\mathbb{E}\left[\mathrm{e}^{\mathrm{j}\omega(\theta(t+\Delta t)-\theta(t))}\right] =$

$$\int_{-\infty}^{\infty} \mathrm{sinc}\left(\frac{\omega}{\pi}\theta_{\rm m}\left(\sin(2\pi q(t+\Delta t)) - \sin(2\pi qt)\right)\right) f_Q(q)\,\mathrm{d}q. \tag{1}$$

*Hardware Impairments.* In practice, all RF transceivers suffer from nonidealities due to their physical characteristics, such as phase noise, I/Q imbalance, and PA nonlinearity [4], which are termed as hardware impairments in this paper. One well-accepted model in the literature is to model the aggregate effect of all hardware impairments as additive and multiplicative distortion noise processes at both the transmitter and receiver [4, Sec. 7.2.2]. In fact, we can write

$$s(t) = \chi_{\rm T}(t)\tilde{s}(t) + \eta_{\rm T}(t), \quad r(t) = \chi_{\rm R}(t)\tilde{r}(t) + \eta_{\rm R}(t), \tag{2}$$

where $\tilde{s}(t)$ (resp. $\tilde{r}(t)$) and $s(t)$ (resp. $r(t)$) are the unimpaired and impaired transmitted (resp. received) signals in complex baseband, respectively, and $\eta_{\rm T}(t)$ and $\chi_{\rm T}(t)$ (resp. $\eta_{\rm R}(t)$ and $\chi_{\rm R}(t)$) are the additive and multiplicative distortion noise processes at the transmitter (resp. receiver), respectively. We assume that these four noise processes are independent from each other and the additive noises are zero-mean. We assume WSS hardware impairments here, which already covers a wide range of scenarios. The more general case of nonstationary processes [4, Sec. 7.2.3] has been tackled in the journal extension [1]. With these assumptions, we model these noise processes using WSS Gaussian processes, which is also supported by measurements [4], [18]. Defining the ACF of WSS random process $X(t)$ as $A_X(t_1,t_2) = \mathbb{E}[X^*(t_1)X(t_2)] = A_X(t_2-t_1)$, we write the ACF of our four noise processes using the squared exponential function [21] as:

$$A_{\eta_{\rm T}}(\Delta t) = \kappa_{\eta_{\rm T}}^2 \mathrm{e}^{-\frac{(\Delta t)^2}{2l_{\eta_{\rm T}}^2}}, \qquad A_{\eta_{\rm R}}(\Delta t) = \kappa_{\eta_{\rm R}}^2 \mathrm{e}^{-\frac{(\Delta t)^2}{2l_{\eta_{\rm R}}^2}}, \tag{3}$$

$$A_{\chi_{\rm T}}(\Delta t) = \kappa_{\chi_{\rm T}}^2 \mathrm{e}^{-\frac{(\Delta t)^2}{2l_{\chi_{\rm T}}^2}}, \qquad A_{\chi_{\rm R}}(\Delta t) = \kappa_{\chi_{\rm R}}^2 \mathrm{e}^{-\frac{(\Delta t)^2}{2l_{\chi_{\rm R}}^2}}, \tag{4}$$

where $\kappa_{\eta_{\rm T}}^2$ and $l_{\eta_{\rm T}}$ are design parameters, which represent the maximum power and the characteristic length-scale of the additive distortion noise process at the transmitter, respectively. The other design parameters ($\kappa_{\eta_{\rm R}}^2$, $\kappa_{\chi_{\rm T}}^2$, $\kappa_{\chi_{\rm R}}^2$, $l_{\eta_{\rm R}}$, $l_{\chi_{\rm T}}$, and $l_{\chi_{\rm R}}$) are defined similarly.

Without hardware impairments, we can write the received signal $\tilde{r}(t)$ and the channel impulse response $\tilde{c}(\tau;t)$ in complex baseband, respectively, as

$$\tilde{r}(t) = \sum_{i=0}^{N} \alpha_i(t)\mathrm{e}^{-\mathrm{j}\varphi_i(t)}\tilde{s}(t-\tau_i(t)) + \tilde{n}(t), \tag{5}$$

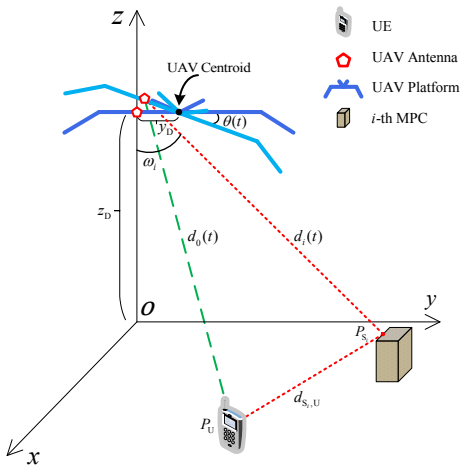


Fig. 1. Spatial setup where the UAV platform wobbles and the UAV transceiver suffers from various hardware impairments.

$$\tilde{c}(\tau;t)=\sum_{i=0}^{N}\alpha_i(t)\mathrm{e}^{-\mathrm{j}\varphi_i(t)}\delta(\tau-\tau_i(t)), \tag{6}$$

where $\tau$ and $t$ are the delay variable and observation time, respectively, $\alpha_i(t)$, $\tau_i(t)$, and $\varphi_i(t)$ are the amplitude, delay, and phase of the $i$-th MPC, respectively, $\tilde{n}(t)$ is the additive white Gaussian noise (AWGN) with PSD of $\frac{N_0}{2}$, and $\delta(.)$ is the Dirac delta function. We provide our assumptions about channel parameters next.

*Amplitude.* We assume that the amplitude does not change noticeably over the time period of interest and follows the well-accepted Laplacian model as [22], [23]

$$|\alpha_i|^2=\frac{1}{2\beta}\mathrm{e}^{-\frac{|\omega_i-\omega_0|}{\beta}},\qquad 1\le i\le N, \tag{7}$$

where $\omega_i\sim U[0,\frac{\pi}{2})$ and $\beta>0$ is a scaling parameter. Thus, the power of the $i$-th MPC can be written as $P_{\alpha_i}\coloneqq\mathbb{E}\left[|\alpha_i|^2\right]=\frac{1}{\pi}(1-\mathrm{e}^{-\frac{\pi}{4\beta}}\cosh(\frac{\omega_0-\pi/4}{\beta}))$. We also assume Rician fading with factor $K$, which gives the power of the LoS component as $P_{\alpha_0}\coloneqq\mathbb{E}\left[|\alpha_0|^2\right]=NKP_{\alpha_1}$.

*Delay.* Similar to the amplitude, we assume that the delay also does not change noticeably over the time period of interest and write it as $\tau_i(t)\approx\tau_i=\frac{d_i(0)+d_{\mathrm{S}_i,\mathrm{U}}}{c}$. Assuming that the UAV only knows the location of the UE, the propagation delay of the $i$-th MPC can be written as $\tau_i=\tau_0+\tau_{\Delta i}$, where $\tau_0=\frac{d_0}{\mathrm{c}}$ is the UAV-UE delay and $\tau_{\Delta i}$ is the excess delay of the $i$-th MPC distributed exponentially with parameter $\rho_i$ [23], [24]. Thus, the pdfs of $\tau_0$ and $\tau_i$ can be written, respectively, as

$$f_{\tau_0}(\tau)=\delta(\tau-\tau_0),\quad f_{\tau_i}(\tau)=\rho_i\mathrm{e}^{-\rho_i(\tau-\tau_0)}\mathbf{1}(\tau-\tau_0), \tag{8}$$

where $1\le i\le N$ and $\mathbf{1}(.)$ is the indicator function.

*Phase.* Unlike amplitude and delay, the phase of the $i$-th MPC changes significantly over time due to UAV wobbling. To see this more clearly, let us first establish a connection between the UAV wobbling pitch angle and the UAV-MPC distances at different times, which is provided next.

**Lemma 1.** *For a wobbling UAV, assuming $\theta(t)\ll 1$ rad and $y_{\mathrm{D}}\ll d_i(t)$, we have*

$$d_i(t+\Delta t)-d_i(t)\approx y_{\mathrm{D}}\cos(\omega_i)[\theta(t+\Delta t)-\theta(t)]. \tag{9}$$

*Proof:* See [3, Lemma 1]. ∎

Following this lemma, we observe a Doppler shift in the channel, which can be written as

$$\varphi_{\mathrm{D}_i}(t,\Delta t)=\frac{2\pi}{\lambda}y_{\mathrm{D}}\cos(\omega_i)[\theta(t+\Delta t)-\theta(t)], \tag{10}$$

where $\lambda=\frac{c}{f_{\mathrm{c}}}$ is the signal wavelength, $c$ is the speed of light, and $f_{\mathrm{c}}$ is the carrier frequency. Therefore, these small distance variations over time become important for the sake of phase as they are multiplied by $f_{\mathrm{c}}$. The phase of the $i$-th MPC can now be written as

$$\begin{aligned}\varphi_i(t)&=\frac{2\pi}{\lambda}\left(d_i(0)+d_{\mathrm{S}_i,\mathrm{U}}\right)+\frac{2\pi}{\lambda}y_{\mathrm{D}}\cos(\omega_i)[\theta(t)-\theta(0)]\\&=2\pi f_{\mathrm{c}}\tau_i+\varphi_{\mathrm{D}_i}(t),\end{aligned} \tag{11}$$

where $\varphi_{\mathrm{D}_i}(t)\coloneqq\varphi_{\mathrm{D}_i}(0,t)$ is the Doppler phase shift at time $t$ given in (10). Defining the ACF of the channel impulse response as $A_{\mathrm{c}}(\tau;t,\Delta t)=\mathbb{E}\left[c^*(\tau;t)c(\tau;t+\Delta t)\right]$, we introduce the metrics discussed in this paper next.

*Coherence Time.* The period of time over which the channel remains almost constant is defined as the coherence time of the channel [25]. Mathematically speaking, we can write [26]

$$T_{\mathrm{Coh}}(t)\coloneqq\min\left\{\Delta t:\frac{|A_{\mathrm{C}}(t,\Delta t)|}{\max|A_{\mathrm{C}}(t,\Delta t)|}\le\gamma_{\mathrm{T}}\right\}, \tag{12}$$

where $A_{\mathrm{C}}(t,\Delta t)=A_{\mathrm{C}}(\Delta f=0;t,\Delta t)$, $\gamma_{\mathrm{T}}$ is a given threshold, and $A_{\mathrm{C}}(\Delta f;t,\Delta t)=\mathcal{F}_\tau\{A_{\mathrm{c}}(\tau;t,\Delta t)\}$, where $\mathcal{F}_\tau\{.\}$ denotes the Fourier transform with respect to $\tau$.

*PSD of Distortion-Plus-Noise.* We refer to all additive distortion noise processes (including the AWGN) as the "distortion-plus-noise" process (see (14)) and evaluate its PSD as our second metric. By definition, the PSD of signal $x(t)$ can be written as $S_x(f)=\mathcal{F}_\tau\{\langle\mathbb{E}[x^*(t)x(t+\Delta t)]\rangle_t\}$, where $\langle y(t)\rangle_t=\lim_{T\to\infty}\frac{1}{2T}\int_{-T}^{T}y(t)\,\mathrm{d}t$ represents time averaging of signal $y(t)$ [27, Sec. 7.2].

## III. Impairments-Aware Unified Channel Model

Let us revisit (5) and (6) considering hardware impairments. From (2), we can write the received signal as

$$\begin{aligned}r(t)&=\chi_{\mathrm{R}}(t)\sum_{i=0}^{N}\alpha_i(t)\mathrm{e}^{-\mathrm{j}\varphi_i(t)}\Big(\chi_{\mathrm{T}}(t-\tau_i(t))\tilde{s}(t-\tau_i(t))\\&\quad+\eta_{\mathrm{T}}(t-\tau_i(t))\Big)+\eta_{\mathrm{R}}(t)+\tilde{n}(t)\\&=\sum_{i=0}^{N}\alpha_i(t)\mathrm{e}^{-\mathrm{j}\varphi_i(t)}\chi_{\mathrm{R}}(t)\chi_{\mathrm{T}}(t-\tau_i(t))\tilde{s}(t-\tau_i(t))+n(t),\end{aligned} \tag{13}$$

where $n(t)$ represents the combined effect of AWGN, UAV wobbling, and hardware impairments, and is given as

$$n(t)=\sum_{i=0}^{N}\alpha_i(t)\mathrm{e}^{-\mathrm{j}\varphi_i(t)}\chi_{\mathrm{R}}(t)\eta_{\mathrm{T}}(t-\tau_i(t))+\eta_{\mathrm{R}}(t)+\tilde{n}(t). \tag{14}$$

From (13), the channel impulse response can be written as

$$c(\tau;t)=\sum_{i=0}^{N}\alpha_i(t)\mathrm{e}^{-\mathrm{j}\varphi_i(t)}\chi_{\mathrm{R}}(t)\chi_{\mathrm{T}}(t-\tau_i(t))\delta(\tau-\tau_i(t)). \tag{15}$$

Note that the impact of UAV wobbling lies in the phase term ($\varphi_i(t)$; see (11)). The new channel impulse response in (15) together with the distortion-plus-noise process in (14) build our air-to-ground impairments-aware unified channel model. The following lemma gives the ACF of the channel impulse response and its Fourier transform.

**Lemma 2.** *In an air-to-ground wireless channel with physical and hardware impairments, where the channel impulse response is given by* (15)*, the channel ACF and its Fourier transform with respect to $\tau$ can be written, respectively, as*

$$\begin{aligned}A_{\mathrm{c}}(\tau;t,\Delta t)&=\sum_{i=0}^{N}A_{\chi_{\mathrm{R}}}(\Delta t)A_{\chi_{\mathrm{T}}}(\Delta t)f_{\tau_i}(\tau)\\&\quad\times\mathbb{E}\Big[|\alpha_i|^2\mathrm{e}^{-\mathrm{j}\frac{2\pi}{\lambda}y_{\mathrm{D}}\cos(\omega_i)[\theta(t+\Delta t)-\theta(t)]}\Big],\end{aligned} \tag{16}$$

$$\begin{aligned}A_{\mathrm{C}}(\Delta f;t,\Delta t)&=\sum_{i=0}^{N}A_{\chi_{\mathrm{R}}}(\Delta t)A_{\chi_{\mathrm{T}}}(\Delta t)\int_0^\infty f_{\tau_i}(\tau)\mathrm{e}^{-\mathrm{j}2\pi\Delta f\tau}\mathrm{d}\tau\\&\quad\times\mathbb{E}\Big[|\alpha_i|^2\mathrm{e}^{-\mathrm{j}\frac{2\pi}{\lambda}y_{\mathrm{D}}\cos(\omega_i)[\theta(t+\Delta t)-\theta(t)]}\Big].\end{aligned} \tag{17}$$

*Proof:* By definition, we can write $A_{\rm c}(\tau;t,\Delta t)$

$$
\begin{aligned}
&= \mathbb{E}\left[c^*(\tau;t)c(\tau;t+\Delta t)\right] \\
&= \mathbb{E}\Bigg[\sum_{i=0}^{N}\sum_{k=0}^{N}\alpha_i^*\alpha_k \mathrm{e}^{-\mathrm{j}(\varphi_k(t+\Delta t)-\varphi_i(t))}\chi_{\rm R}^*(t)\chi_{\rm R}(t+\Delta t) \\
&\quad \times \chi_{\rm T}^*(t-\tau_i)\chi_{\rm T}(t-\tau_k+\Delta t)\delta(\tau-\tau_i)\delta(\tau-\tau_k)\Bigg] \\
&= \sum_{i=0}^{N}\sum_{\substack{k=0\\k\neq i}}^{N}\mathbb{E}\Big[\alpha_i^*\alpha_k \mathrm{e}^{-\mathrm{j}\frac{2\pi}{\lambda}\left(d_k(0)+d_{\mathrm{S}_k,\mathrm{U}}-d_i(0)-d_{\mathrm{S}_i,\mathrm{U}}\right)} \\
&\quad \times \mathrm{e}^{-\mathrm{j}\left(\varphi_{\mathrm{D}_k}(t+\Delta t)-\varphi_{\mathrm{D}_i}(t)\right)}\chi_{\rm R}^*(t)\chi_{\rm R}(t+\Delta t) \\
&\quad \times \chi_{\rm T}^*(t-\tau_i)\chi_{\rm T}(t-\tau_k+\Delta t)\delta(\tau-\tau_i)\delta(\tau-\tau_k)\Big] \\
&\quad + \sum_{i=0}^{N}\mathbb{E}\Big[|\alpha_i|^2\mathrm{e}^{-\mathrm{j}\left(\varphi_{\mathrm{D}_i}(t+\Delta t)-\varphi_{\mathrm{D}_i}(t)\right)}\chi_{\rm R}^*(t)\chi_{\rm R}(t+\Delta t) \\
&\quad \times \chi_{\rm T}^*(t-\tau_i)\chi_{\rm T}(t-\tau_i+\Delta t)\delta(\tau-\tau_i)\delta(\tau-\tau_i)\Big].
\end{aligned}
$$

Since $d_{\mathrm{S}_k,\mathrm{U}} - d_{\mathrm{S}_i,\mathrm{U}} \gg \lambda$, we note that $X_{k,i} = \left[\frac{2\pi}{\lambda}\left(d_{\mathrm{S}_k,\mathrm{U}} - d_{\mathrm{S}_i,\mathrm{U}}\right) \bmod 2\pi\right] \sim U[0,2\pi)$ [28, Lemma 4], which gives $\mathbb{E}\left[\mathrm{e}^{-\mathrm{j}X_{k,i}}\right] = 0$. Thus, the double-summation in the last equality becomes zero. As for the single summation, we encounter the singularity issue (delta squared), which can be avoided by isolating one of the delta functions [29] and rewriting the channel ACF with only one delta function as

$$
\begin{aligned}
A_{\rm c}(\tau;t,\Delta t) &= \sum_{i=0}^{N}\mathbb{E}\Big[|\alpha_i|^2\mathrm{e}^{-\mathrm{j}\frac{2\pi}{\lambda}y_{\rm D}\cos(\omega_i)[\theta(t+\Delta t)-\theta(t)]} \\
&\quad \times \chi_{\rm R}^*(t)\chi_{\rm R}(t+\Delta t)\chi_{\rm T}^*(t-\tau_i)\chi_{\rm T}(t-\tau_i+\Delta t)\delta(\tau-\tau_i)\Big] \\
&= \sum_{i=0}^{N}\int_{-\infty}^{\infty}\mathbb{E}\left[|\alpha_i|^2\mathrm{e}^{-\mathrm{j}\frac{2\pi}{\lambda}y_{\rm D}\cos(\omega_i)[\theta(t+\Delta t)-\theta(t)]}\right] \\
&\quad \times A_{\chi_{\rm R}}(\Delta t)A_{\chi_{\rm T}}(\Delta t)\delta(\tau-\tau_i)f_{\tau_i}(\tau_i)\,\mathrm{d}\tau_i,
\end{aligned}
$$

which gives the result in (16) by applying the sifting property of the delta function. The result in (17) is obtained simply by taking the Fourier transform of (16) with respect to $\tau$. ∎

Equipped with the channel ACF, we can now derive the coherence time of the channel by setting $\Delta f = 0$ in (17). This result if formally presented next.

**Theorem 1.** *The coherence time of the impairments-aware air-to-ground wireless channel is given in* (12)*, where the channel ACF can be written as*

$$
\begin{aligned}
A_{\rm C}(t,\Delta t) &= \sum_{i=0}^{N}A_{\chi_{\rm R}}(\Delta t)A_{\chi_{\rm T}}(\Delta t) \\
&\quad \times \mathbb{E}\left[|\alpha_i|^2\mathrm{e}^{-\mathrm{j}\frac{2\pi}{\lambda}y_{\rm D}\cos(\omega_i)[\theta(t+\Delta t)-\theta(t)]}\right]. \quad (18)
\end{aligned}
$$

Note that Theorem 1 is valid for any WSS distortion noise process as well as for any UAV wobbling model. Given that, we intend to simplify it further for the specific case studies mentioned earlier in Section II to obtain useful insights. Let us first evaluate the expectation that involves the impact of UAV wobbling as follows:

$$
\begin{aligned}
G_i(t,\Delta t) &= \mathbb{E}\left[|\alpha_i|^2\mathrm{e}^{-\mathrm{j}\frac{2\pi}{\lambda}y_{\rm D}\cos(\omega_i)[\theta(t+\Delta t)-\theta(t)]}\right] \\
&= \begin{cases}
\int_0^{\pi/2}\int_{-\infty}^{\infty}\frac{1}{\pi\beta}\mathrm{e}^{-\frac{|\omega_i-\omega_0|}{\beta}}f_Q(q)\,\mathrm{sinc}\Big(\frac{2}{\lambda}\theta_{\rm m}y_{\rm D}\cos(\omega_i) \\
\quad \times(\sin(2\pi q(t+\Delta t))-\sin(2\pi qt))\Big)\mathrm{d}q\,\mathrm{d}\omega_i, & i\neq 0 \\
2NKP_{\alpha_1}\int_{-\infty}^{\infty}f_Q(q)\,\mathrm{sinc}\Big(\frac{2}{\lambda}\theta_{\rm m}y_{\rm D}\cos(\omega_0) \\
\quad \times(\sin(2\pi q(t+\Delta t))-\sin(2\pi qt))\Big)\mathrm{d}q, & i=0,
\end{cases} \quad (19)
\end{aligned}
$$

where the functions $G_i(t,\Delta t),\ 1\le i\le N$ are all equal to each other. Using this function and the Gaussian multiplicative distortion noise processes defined in (4), we can simplify the ACF given in Theorem 1 as $A_{\rm C}(t,\Delta t) =$

$$
\kappa_{\chi_{\rm R}}^2\kappa_{\chi_{\rm T}}^2\mathrm{e}^{-\left(\frac{1}{2l_{\chi_{\rm R}}^2}+\frac{1}{2l_{\chi_{\rm T}}^2}\right)(\Delta t)^2}\left(G_0(t,\Delta t)+NG_1(t,\Delta t)\right).
$$

Since the maximum value of this ACF is $2\kappa_{\chi_{\rm R}}^2\kappa_{\chi_{\rm T}}^2N(K+1)P_{\alpha_1}$, the coherence time can be written as

$$
\begin{aligned}
T_{\rm Coh}^{\rm WSS}(t) = \min\Bigg\{\Delta t : &\frac{\mathrm{e}^{-\left(\frac{1}{2l_{\chi_{\rm R}}^2}+\frac{1}{2l_{\chi_{\rm T}}^2}\right)(\Delta t)^2}}{2N(K+1)P_{\alpha_1}} \\
&\times |G_0(t,\Delta t)+NG_1(t,\Delta t)| \le \gamma_{\rm T}\Bigg\}, \quad (20)
\end{aligned}
$$

which should be solved numerically for $\Delta t$.

In order to study the behavior of the effective received noise at the ground UE, we analyze the PSD of $n(t)$ as defined in (14), which is the AWGN plus the aggregate distortion caused by physical and hardware impairments at both the transmitter and the receiver. The following theorem provides this result.

**Theorem 2.** *The PSD of the distortion-plus-noise process $n(t)$ can be written as*

$$
\begin{aligned}
S_n(f) = \frac{N_0}{2} &+ \mathcal{F}_{\Delta t}\{A_{\eta_{\rm R}}(\Delta t)\} + \sum_{i=0}^{N}\mathcal{F}_{\Delta t}\Bigg\{A_{\chi_{\rm R}}(\Delta t)A_{\eta_{\rm T}}(\Delta t) \\
&\times\left\langle\mathbb{E}\left[|\alpha_i|^2\mathrm{e}^{-\mathrm{j}\frac{2\pi}{\lambda}y_{\rm D}\cos(\omega_i)[\theta(t+\Delta t)-\theta(t)]}\right]\right\rangle_t\Bigg\}. \quad (21)
\end{aligned}
$$

*Proof:* By definition, the ACF of $n(t)$ can be written as

$$
\begin{aligned}
A_n(t,t+\Delta t) &= \mathbb{E}\left[n^*(t)n(t+\Delta t)\right] \\
&\overset{(a)}{=} \mathbb{E}\left[\tilde{n}^*(t)\tilde{n}(t+\Delta t)\right] + \mathbb{E}\left[\eta_{\rm R}^*(t)\eta_{\rm R}(t+\Delta t)\right] \\
&\quad + \mathbb{E}\Bigg[\Bigg(\sum_{i=0}^{N}\alpha_i^*\mathrm{e}^{\mathrm{j}\varphi_i(t)}\chi_{\rm R}^*(t)\eta_{\rm T}^*(t-\tau_i(t))\Bigg)\Bigg(\sum_{i=0}^{N}\alpha_i \\
&\quad \times \mathrm{e}^{-\mathrm{j}\varphi_i(t+\Delta t)}\chi_{\rm R}(t+\Delta t)\eta_{\rm T}(t+\Delta t-\tau_i(t+\Delta t))\Bigg)\Bigg] \\
&\overset{(b)}{=} A_{\tilde{n}}(\Delta t) + A_{\eta_{\rm R}}(\Delta t) + \mathbb{E}\Bigg[\sum_{i=0}^{N}|\alpha_i|^2\mathrm{e}^{-\mathrm{j}(\varphi_i(t+\Delta t)-\varphi_i(t))} \\
&\quad \times \chi_{\rm R}^*(t)\chi_{\rm R}(t+\Delta t)\eta_{\rm T}^*(t-\tau_i)\eta_{\rm T}(t-\tau_i+\Delta t)\Bigg] \\
&= A_{\tilde{n}}(\Delta t) + A_{\eta_{\rm R}}(\Delta t) + \sum_{i=0}^{N}A_{\chi_{\rm R}}(\Delta t)A_{\eta_{\rm T}}(\Delta t) \\
&\quad \times \mathbb{E}\left[|\alpha_i|^2\mathrm{e}^{-\mathrm{j}\frac{2\pi}{\lambda}y_{\rm D}\cos(\omega_i)[\theta(t+\Delta t)-\theta(t)]}\right], \quad (22)
\end{aligned}
$$

where in $(a)$ we used $\mathbb{E}[\eta_{\rm R}(t)] = \mathbb{E}[\tilde{n}(t)] = 0$ and the independence between distortion noises and the AWGN, and

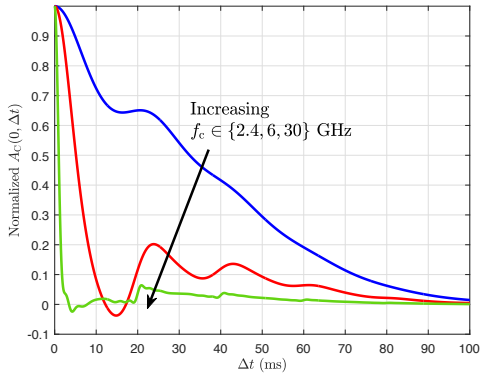


Fig. 2. Normalized channel ACF to obtain coherence time for different $f_c$. Assumptions: $\theta_m = 5°$, and $l_{\chi_T} = l_{\chi_R} = 0.05$ s.

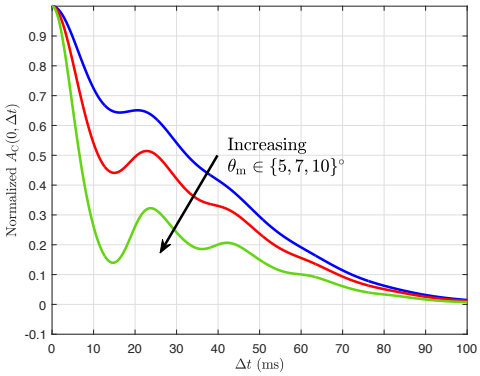


Fig. 3. Normalized channel ACF to obtain coherence time for different $\theta_m$. Assumptions: $f_c = 2.4$ GHz, and $l_{\chi_T} = l_{\chi_R} = 0.05$ s.

in $(b)$ we used the fact that the cross terms in the double-summation are zero (see the proof of Lemma 2). Since $\tilde{n}(t)$ is a white process, we have $A_{\tilde{n}}(\Delta t) = \frac{N_0}{2}\delta(\Delta t)$. The final result in (21) is obtained by first averaging (22) over $t$ and then taking its Fourier transform with respect to $\Delta t$. ■

Theorem 2 gives the PSD of $n(t)$ for the general case. However, similar to our analysis for the channel coherence time, we simplify this result for the case studies provided in Section II to gain further insights. For that, we need to also average $G_i(t, \Delta t)$ over $t$. We can write the PSD of $n(t)$ as

$$
\begin{aligned}
S_n(f) &= \frac{N_0}{2} + \mathcal{F}_{\Delta t}\left\{\kappa^2_{\eta_R} \mathrm{e}^{-\frac{(\Delta t)^2}{2l^2_{\eta_R}}}\right\} \\
&\quad + \sum_{i=0}^{N} \mathcal{F}_{\Delta t}\left\{\kappa^2_{\chi_R} \mathrm{e}^{-\frac{(\Delta t)^2}{2l^2_{\chi_R}}} \kappa^2_{\eta_T} \mathrm{e}^{-\frac{(\Delta t)^2}{2l^2_{\eta_T}}} \left\langle G_i^{\mathrm{NonSI}}(t, \Delta t)\right\rangle_t\right\} \\
&= \frac{N_0}{2} + \kappa^2_{\eta_R}\sqrt{2\pi l^2_{\eta_R}} \mathrm{e}^{-2\pi^2 l^2_{\eta_R} f^2} \\
&\quad + 2P_{\alpha_0} \lim_{T\to\infty} \frac{1}{T} \int_0^T \int_{-\infty}^{\infty} \int_{-\infty}^{\infty} \kappa^2 \mathrm{e}^{-\frac{(\Delta t)^2}{2l^2}} \\
&\qquad \times \mathrm{sinc}\left(\frac{2}{\lambda}\theta_m y_D \cos(\omega_0)\left(\sin(2\pi q(t+\Delta t)) - \sin(2\pi q t)\right)\right) \\
&\qquad \times f_Q(q)\, \mathrm{e}^{-\mathrm{j}2\pi f \Delta t}\, \mathrm{d}q\, \mathrm{d}\Delta t\, \mathrm{d}t \\
&\quad + N \lim_{T\to\infty} \frac{1}{T} \int_0^T \int_{-\infty}^{\infty} \int_0^{\frac{\pi}{2}} \int_{-\infty}^{\infty} \kappa^2 \mathrm{e}^{-\frac{(\Delta t)^2}{2l^2}} \frac{1}{\pi\beta} \mathrm{e}^{-\frac{|\omega_i - \omega_0|}{\beta}} \\
&\qquad \times \mathrm{sinc}\left(\frac{2}{\lambda}\theta_m y_D \cos(\omega_i)\left(\sin(2\pi q(t+\Delta t)) - \sin(2\pi q t)\right)\right) \\
&\qquad \times f_Q(q)\, \mathrm{e}^{-\mathrm{j}2\pi f \Delta t}\, \mathrm{d}q\, \mathrm{d}\omega_i\, \mathrm{d}\Delta t\, \mathrm{d}t, \qquad (23)
\end{aligned}
$$

where $\kappa^2 = \kappa^2_{\chi_R}\kappa^2_{\eta_T}$ and $l^{-2} = l^{-2}_{\chi_R} + l^{-2}_{\eta_T}$. In the last equality, we used the definition of Fourier transform, swapped the order of limit and integral, and used the Fourier transform of a Gaussian function, i.e., $\mathcal{F}_x\{\mathrm{e}^{-ax^2}\} = \sqrt{\frac{\pi}{a}}\mathrm{e}^{-\frac{\pi^2}{a}f^2}$.

## IV. Numerical Results

In this section, we present numerical results to glean further insights from our analyses in the previous sections. The simulation parameters are as follows: $N \in \{10, 20\}$ for mmWave and sub-6 GHz frequencies, respectively, $f_c \in \{2.4, 6, 30\}$ GHz (thus, $\lambda \in \{12.5, 5, 1\}$ cm), $y_D = 40$ cm, $\omega_0 = 20°$, $K = 11.5$ [30, Table 1], $\beta = 1$, $N_0 = 10^{-8}$ W, $\theta_m \in \{5, 7, 10\}°$ [20], $Q \sim U[5, 25)$, $\{\kappa^2_{\eta_T}, \kappa^2_{\eta_R}, \kappa^2_{\chi_T}, \kappa^2_{\chi_R}\} \in \{0.1, 0.5, 1\}$ W, and $\{l_{\eta_T}, l_{\eta_R}, l_{\chi_T}, l_{\chi_R}\} \in \{0.01, 0.05, 0.1\}$ s.

The impact of different impairments on the channel coherence time is depicted in Figs. 2 and 3. As seen from (11) and (13), $\varphi_i(t)$ depends on the carrier frequency and the UAV-UE distance. Hence, increasing $f_c$ or $\theta_m$ (thereby, the UAV-UE distance) results in higher channel variations, which, in turn, decreases the channel coherence time. From these figures, we see that $T_{\mathrm{Coh}} = \{32.52, 5.13, 0.98\}$ ms for $f_c = \{2.4, 6, 30\}$ GHz and $\theta_m = 5°$ and $T_{\mathrm{Coh}} = \{32.52, 11.13, 6.63\}$ ms for $\theta_m = \{5, 7, 10\}°$ and $f_c = 2.4$ GHz. These numbers show the degradation of channel coherence time with UAV wobbling and hardware impairments, especially at larger $\theta_m$ and higher $f_c$ (mmWave and higher), which makes it difficult to establish reliable aerial-terrestrial communications links.

Numerical results for the PSD of $n(t)$ are provided in Figs. 4 and 5. The impact of hardware impairment intensity on the PSD of $n(t)$ is shown in Fig. 4, where increasing the maximum power of hardware impairments ($\kappa^2$ parameters) while keeping their characteristic length-scales constant ($l$ parameters) increases the total power of $n(t)$ (shifts the PSD upward). Conversely, decreasing $l$ while keeping $\kappa^2$ constant flattens the PSD curve, which could either decrease or increase the total power of $n(t)$ depending on the specific values of $l$ and $\kappa^2$. We compare the PSD of $n(t)$ for different values of the maximum UAV pitch angle in Fig. 5, where we observe that for realistic values of $\theta_m$, the PSD of $n(t)$ does not change noticeably with increasing $\theta_m$.

## V. Conclusion

In this paper, we provided a unified channel model for the air-to-ground wireless communication link between a UAV and a ground UE that suffer from various impairments. We studied two different types of nonidealities: (i) physical impairments caused by UAV wobbling, and (ii) hardware impairments caused by RF nonidealities at both the UAV and the UE. Specifically, we modeled UAV wobbling by sinusoidal stochastic processes to demonstrate the oscillatory nature of wobbling, and modeled the aggregate impact of all hardware impairments by two WSS additive and multiplicative distortion noise processes. Using these well-accepted models,

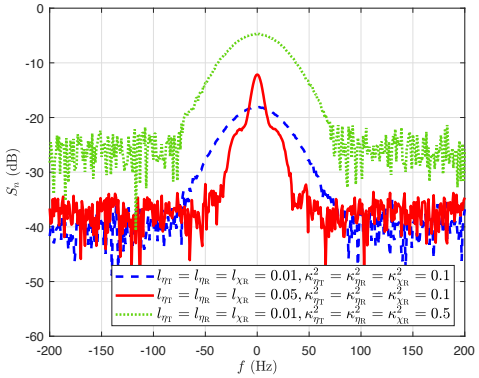


Fig. 4. PSD of $n(t)$ for different impairment levels. Assumptions: $N = 20$, $f_c = 2.4$ GHz, and $\theta_m = 5°$.

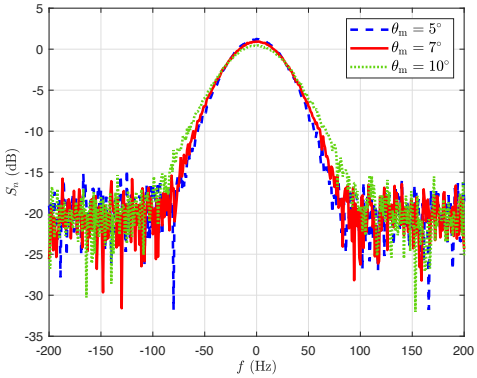


Fig. 5. PSD of $n(t)$ for different $\theta_m$. Assumptions: $N = 20$, $f_c = 2.4$ GHz, $\kappa^2_{\eta_T} = \kappa^2_{\eta_R} = \kappa^2_{\chi_R} = 1$ W, and $l_{\eta_T} = l_{\eta_R} = l_{\chi_R} = 0.01$ s.

we rigorously derived the channel impulse response ACF, from which we obtained the coherence time of the channel and the PSD of the distortion-plus-noise process as our key channel metrics. The analysis presented in this paper demonstrated that the channel coherence time degrades quickly at high carrier frequencies due to UAV wobbling and hardware impairments, rendering channel estimation in aerial-terrestrial links extremely challenging at mmWave and higher frequencies. To the best of our knowledge, this is the first work that provides a unified channel model that accounts for the joint impact of UAV wobbling and hardware impairments on the air-to-ground channel. One extension of this work is to study the joint impact of physical and hardware impairments on a wireless channel where either the UAV or the UE is *mobile*, which will complicate further the calculation of the effective Doppler phase shift.

## REFERENCES


[1] M. Banagar and H. S. Dhillon, "Fundamentals of wobbling and hardware impairments-aware air-to-ground channel model," *submitted to IEEE Trans. Wireless Commun.*, [Online]. Available: https://arxiv.org/abs/2205.10957.

[2] M. Mozaffari *et al.*, "A tutorial on UAVs for wireless networks: Applications, challenges, and open problems," *IEEE Commun. Surveys Tuts.*, vol. 21, no. 3, pp. 2334–2360, 3rd Quart. 2019.

[3] M. Banagar, H. S. Dhillon, and A. F. Molisch, "Impact of UAV wobbling on the air-to-ground wireless channel," *IEEE Trans. Veh. Technol.*, vol. 69, no. 11, pp. 14 025–14 030, Nov. 2020.

[4] T. Schenk, *RF Imperfections in High-Rate Wireless Systems: Impact and Digital Compensation*. Springer, 2008.

[5] E. Bjornson *et al.*, "Massive MIMO systems with non-ideal hardware: Energy efficiency, estimation, and capacity limits," *IEEE Trans. Inf. Theory*, vol. 60, no. 11, pp. 7112–7139, Nov. 2014.

[6] W. Khawaja *et al.*, "A survey of air-to-ground propagation channel modeling for unmanned aerial vehicles," *IEEE Commun. Surveys Tuts.*, vol. 21, no. 3, pp. 2361–2391, 3rd Quart. 2019.

[7] A. Al-Hourani, S. Kandeepan, and S. Lardner, "Optimal LAP altitude for maximum coverage," *IEEE Wireless Commun. Lett.*, vol. 3, no. 6, pp. 569–572, Dec. 2014.

[8] X. Cai *et al.*, "An empirical air-to-ground channel model based on passive measurements in LTE," *IEEE Trans. Veh. Technol.*, vol. 68, no. 2, pp. 1140–1154, Feb. 2019.

[9] J. Sabzehali, V. K. Shah, H. S. Dhillon, and J. H. Reed, "3D placement and orientation of mmWave-based UAVs for guaranteed LoS coverage," *IEEE Wireless Commun. Lett.*, vol. 10, no. 8, pp. 1662–1666, Aug. 2021.

[10] 3GPP, "Study on enhanced LTE support for aerial vehicles," 3rd Generation Partnership Project (3GPP), Tech. Rep. 36.777, 01 2018.

[11] M. T. Dabiri *et al.*, "Analytical channel models for millimeter wave UAV networks under hovering fluctuations," *IEEE Trans. Wireless Commun.*, vol. 19, no. 4, pp. 2868–2883, Apr. 2020.

[12] D. Xu, Y. Sun, D. W. K. Ng, and R. Schober, "Multiuser MISO UAV communications in uncertain environments with no-fly zones: Robust trajectory and resource allocation design," *IEEE Trans. Commun.*, vol. 68, no. 5, pp. 3153–3172, May 2020.

[13] S. Yang, Z. Zhang, J. Zhang, and J. Zhang, "Impact of rotary-wing UAV wobbling on millimeter-wave air-to-ground wireless channel," *arXiv preprint*, [Online]. Available: https://arxiv.org/abs/2107.06461.

[14] J. Gomez-Ponce *et al.*, "Air-to-ground directional channel sounder with drone and 64-antenna dual-polarized cylindrical array," in *Proc. IEEE Int. Conf. Commun. (ICC) Workshops*, June 2021.

[15] T. C. W. Schenk, P. F. M. Smulders, and E. R. Fledderus, "Impact of nonlinearities in multiple-antenna OFDM transceivers," in *Symp. Commun. Veh. Technol.*, Nov. 2006, pp. 53–56.

[16] L. Piazzo and P. Mandarini, "Analysis of phase noise effects in OFDM modems," *IEEE Trans. Commun.*, vol. 50, no. 10, pp. 1696–1705, Oct. 2002.

[17] M. Banagar and H. S. Dhillon, "3D two-hop cellular networks with wireless backhauled UAVs: Modeling and fundamentals," *IEEE Trans. Wireless Commun.*, to appear.

[18] E. Bjornson, M. Matthaiou, and M. Debbah, "A new look at dual-hop relaying: Performance limits with hardware impairments," *IEEE Trans. Commun.*, vol. 61, no. 11, pp. 4512–4525, Nov. 2013.

[19] X. Li *et al.*, "UAV-aided multi-way NOMA networks with residual hardware impairments," *IEEE Wireless Commun. Lett.*, vol. 9, no. 9, pp. 1538–1542, Sep. 2020.

[20] B. Ahmed, H. R. Pota, and M. Garratt, "Flight control of a rotary wing UAV using adaptive backstepping," *Int. J. Robust Nonlinear Control*, vol. 20, no. 6, pp. 639–658, Apr. 2010.

[21] C. E. Rasmussen and C. K. I. Williams, *Gaussian Processes for Machine Learning*. MIT Press, 2006.

[22] K. I. Pedersen, P. E. Mogensen, and B. H. Fleury, "Power azimuth spectrum in outdoor environments," *Electronics Lett.*, vol. 33, no. 18, pp. 1583–1584, Aug. 1997.

[23] A. F. Molisch, *Wireless Communications*. Wiley-IEEE Press, 2011.

[24] C. E. O'Lone, H. S. Dhillon, and R. M. Buehrer, "Characterizing the first-arriving multipath component in 5G millimeter wave networks: TOA, AOA, and non-line-of-sight bias," *IEEE Trans. Wireless Commun.*, vol. 21, no. 3, pp. 1602–1620, Mar. 2022.

[25] A. Goldsmith, *Wireless Communications*. Cambridge University Press, 2005.

[26] V. Va and R. W. Heath, "Basic relationship between channel coherence time and beamwidth in vehicular channels," in *Proc. IEEE 82nd Veh. Technol. Conf. (VTC'15-Fall)*, Sep. 2015.

[27] J. P. Z. Peebles, *Probability, Random Variables, and Random Signal Principles*, 4th ed. McGraw-Hill, Inc., 2001.

[28] H. S. Dhillon and G. Caire, "Wireless backhaul networks: Capacity bound, scalability analysis and design guidelines," *IEEE Trans. Wireless Commun.*, vol. 14, no. 11, pp. 6043–6056, Nov. 2015.

[29] A. Meijerink and A. F. Molisch, "On the physical interpretation of the Saleh-Valenzuela model and the definition of its power delay profiles," *IEEE Trans. Antennas Propag.*, vol. 62, no. 9, pp. 4780–4793, Sep. 2014.

[30] N. Goddemeier and C. Wietfeld, "Investigation of air-to-air channel characteristics and a UAV specific extension to the Rice model," in *Proc. IEEE Global Commun. Conf. (Globecom) Workshops*, 2015.